Editor's Summary

Go CAR-Ts in the Fast Lane

As members of the body's police force, cells of the immune system vigilantly pursue bad actors that harm healthy tissues, such as infection or cancer, and then try to deter dangerous activity. Researchers have long sought to harness the power of the immune system to fight cancers such as leukemia; however, targeting functional immune T cells to the tumor and maintaining these cells in patients remains challenging. Now, Kalos *et al.* have genetically modified T cells to express a chimeric antigen receptor (CAR) to yield so-called CAR T cells that specifically target chronic lymphocytic leukemia (CLL) (a B cell cancer). The designer T cells not only expanded, persisted, and attacked tumor cells after transfer into patients; they also mediated cancer remission. Innocent bystanders were also targeted, as reflected by decreased numbers of B cells and plasma cells and the development of hypogammaglobulinemia.

The CAR T cells used in this study expressed an antigen receptor that consists of antibody binding domains that bind in a restricted manner to the CD19 protein (which is found solely on normal B cells and plasma cells) attached to both a T cell–specific costimulatory domain and a T cell–specific intracellular signaling domain. The resulting chimeric receptor could activate T cells in response to CD19 in the absence of major histocompatibility complex restriction, allowing for much broader cellular targeting than is obtained with normal T cells. After transfer into three CLL patients, these CAR T cells expanded >1000-fold, persisted for more than 6 months, and eradicated CLL cells. Some of these CAR T cells persisted with a memory phenotype, which would allow them to respond more quickly and on a larger scale with a second exposure to CLL cells. Indeed, two of the three CLL patients who underwent the CAR T cell treatment had complete remission of their leukemia. Although this is early in the clinical study, these results highlight the potential for CAR-modified T cells to bring cancer therapy up to speed.

LEUKEMIA

T Cells with Chimeric Antigen Receptors Have Potent Antitumor Effects and Can Establish Memory in Patients with Advanced Leukemia

Michael Kalos,[1,2]* Bruce L. Levine,[1,2]* David L. Porter,[1,3] Sharyn Katz,[4] Stephan A. Grupp,[5,6] Adam Bagg,[1,2] Carl H. June[1,2]†

Tumor immunotherapy with T lymphocytes, which can recognize and destroy malignant cells, has been limited by the ability to isolate and expand T cells restricted to tumor-associated antigens. Chimeric antigen receptors (CARs) composed of antibody binding domains connected to domains that activate T cells could overcome tolerance by allowing T cells to respond to cell surface antigens; however, to date, lymphocytes engineered to express CARs have demonstrated minimal in vivo expansion and antitumor effects in clinical trials. We report that CAR T cells that target CD19 and contain a costimulatory domain from CD137 and the T cell receptor ζ chain have potent non–cross-resistant clinical activity after infusion in three of three patients treated with advanced chronic lymphocytic leukemia (CLL). The engineered T cells expanded >1000-fold in vivo, trafficked to bone marrow, and continued to express functional CARs at high levels for at least 6 months. Evidence for on-target toxicity included B cell aplasia as well as decreased numbers of plasma cells and hypogammaglobulinemia. On average, each infused CAR-expressing T cell was calculated to eradicate at least 1000 CLL cells. Furthermore, a CD19-specific immune response was demonstrated in the blood and bone marrow, accompanied by complete remission, in two of three patients. Moreover, a portion of these cells persisted as memory CAR^{+} T cells and retained anti-CD19 effector functionality, indicating the potential of this major histocompatibility complex–independent approach for the effective treatment of B cell malignancies.

INTRODUCTION

Using gene transfer technologies, T cells can be genetically modified to stably express antibody binding domains on their surface that confer novel antigen specificities that are major histocompatibility complex (MHC)–independent. Chimeric antigen receptors (CARs) are an application of this approach that combines an antigen recognition domain of a specific antibody with an intracellular domain of the CD3-ζ chain or FcγRI protein into a single chimeric protein (1, 2). Trials testing CARs are presently under way at a number of academic medical centers (3, 4). In most cancers, tumor-specific antigens are not yet well defined, but in B cell malignancies, CD19 is an attractive tumor target. Expression of CD19 is restricted to normal and malignant B cells (5), and CD19 is a widely accepted target to safely test CARs. Although CARs can trigger T cell activation in a manner similar to an endogenous T cell receptor, a major impediment to the clinical application of this technology to date has been the limited in vivo expansion of CAR^{+} T cells, rapid disappearance of the cells after infusion, and disappointing clinical activity (4, 6).

CAR-mediated T cell responses may be further enhanced with addition of costimulatory domains. In a preclinical model, we found that inclusion of the CD137 (4-1BB) signaling domain significantly increased antitumor activity and in vivo persistence of CARs compared to inclusion of the CD3-ζ chain alone (7, 8). To evaluate the safety and feasibility for adoptive transfer of T cells gene-modified to express such CARs, we initiated a pilot clinical trial using autologous T cells expressing an anti-CD19 CAR including both CD3-ζ and the 4-1BB costimulatory domain (CART19 cells) to target CD19^{+} malignancies. To date, we have treated three patients under this protocol. Some of the findings from one of these patients are described in (9), which reports that this treatment results in tumor regression, CART19 cell persistence, and the unexpected occurrence of delayed tumor lysis syndrome. Here, we show that the CART19 cells mediated potent clinical antitumor effects in all three patients treated. On average, each infused CAR T cell and/or their progeny eliminated more than 1000 leukemia cells in vivo in patients with advanced chemotherapy-resistant chronic lymphocytic leukemia (CLL). CART19 cells underwent robust in vivo T cell expansion, persisted at high levels for at least 6 months in blood and bone marrow (BM), continued to express functional receptors on cells with a memory phenotype, and maintained anti-CD19 effector function in vivo.

RESULTS

Clinical protocol

Three patients with advanced, chemotherapy-resistant CLL were enrolled in a pilot clinical trial for CART19 cell therapy. Figure 1 presents a summary of the manufacturing process for the gene-modified T cells (A) and the clinical protocol design (B). All patients were extensively pretreated with various chemotherapy and biologic regimens (Table 1). Two of the patients had p53-deficient CLL, a deletion that portends poor response to conventional therapy and rapid progression (10). Each of the patients had a large tumor burden after the preparative

[1]Abramson Cancer Center, University of Pennsylvania, Philadelphia, PA 19104, USA. [2]Department of Pathology and Laboratory Medicine, University of Pennsylvania, Philadelphia, PA 19104, USA. [3]Department of Medicine, University of Pennsylvania, Philadelphia, PA 19104, USA. [4]Department of Radiology, University of Pennsylvania, Philadelphia, PA 19104, USA. [5]Department of Pediatrics, University of Pennsylvania, Philadelphia, PA 19104, USA. [6]Division of Oncology, Children's Hospital of Philadelphia, Philadelphia, PA 19104, USA.
*These authors contributed equally to this work.
†To whom correspondence should be addressed. E-mail: cjune@exchange.upenn.edu

chemotherapy, including extensive BM infiltration (40 to 95%) and lymphadenopathy; UPN 02 also had peripheral lymphocytosis. There was a low abundance of T cells in the apheresis products (2.29 to 4.46%) (table S1) as well as likely impaired T cell activation, as has been shown previously in CLL patients (11). Additional details of the cell manufacturing and product characterization for the CART19 cell preparation for each patient are shown in table S1. All patients were pretreated 1 to 4 days before CART19 cell infusions with lymphodepleting chemotherapy (Table 1). A split-dose cell infusion schedule was used to address potential safety concerns related to the evaluation of a previously untested CAR that incorporated the 4-1BB costimulatory signaling domain.

In vivo expansion, persistence, and BM trafficking of CART19 cells

Our preclinical data in two animal models, including mice bearing xenografts of primary human precursor-B acute lymphoblastic leukemia (7, 8), indicated that CAR+ T cells that express a 4-1BB signaling domain expanded after stimulation with anti-CD3/anti-CD28 monoclonal antibody–coated beads (12) and had improved persistence compared to CAR+ T cells lacking 4-1BB. We developed a quantitative polymerase chain reaction (qPCR) assay to enable quantitative tracking of CART19 cells in blood and BM. CART19 cells expanded and persisted in the blood of all patients for at least 6 months (Fig. 2, A and B). Moreover, CART19 cells expanded 1000- to 10,000-fold in the blood of patients UPN 01 and 03 during the first month after infusion, reaching peak frequencies of 10 to >95% of circulating white blood cells in UPN 01 and 03 (Fig. 2C). The peak expansion levels coincided with onset of the clinical symptoms after infusion in UPN 01 (day 15) and UPN 03 (day 23). Furthermore, after an initial decay, which can be modeled with first-order kinetics, the CART19 cell numbers stabilized in all three patients from days 90 to 180 after infusion (Fig. 2B). The CART19 cells also trafficked to the BM in all patients, albeit in 5- to 10-fold fewer numbers than observed in blood (Fig. 2D). CART19 cells had a log-linear decay in the BM in UPN 01 and 03, with a disappearance half-life of ~35 days.

Induction of specific immune responses in the peripheral blood and BM compartments after CART19 infusion

Peripheral blood (PB) and BM serum samples from all patients were collected and batch-analyzed to quantitatively determine cytokine levels. A panel of 30 cytokines, chemokines, and other soluble factors were assessed for potential toxicities and to provide evidence of CART19 cell function. The full data set for all of the cytokines measured in each of the three patients through the date of this
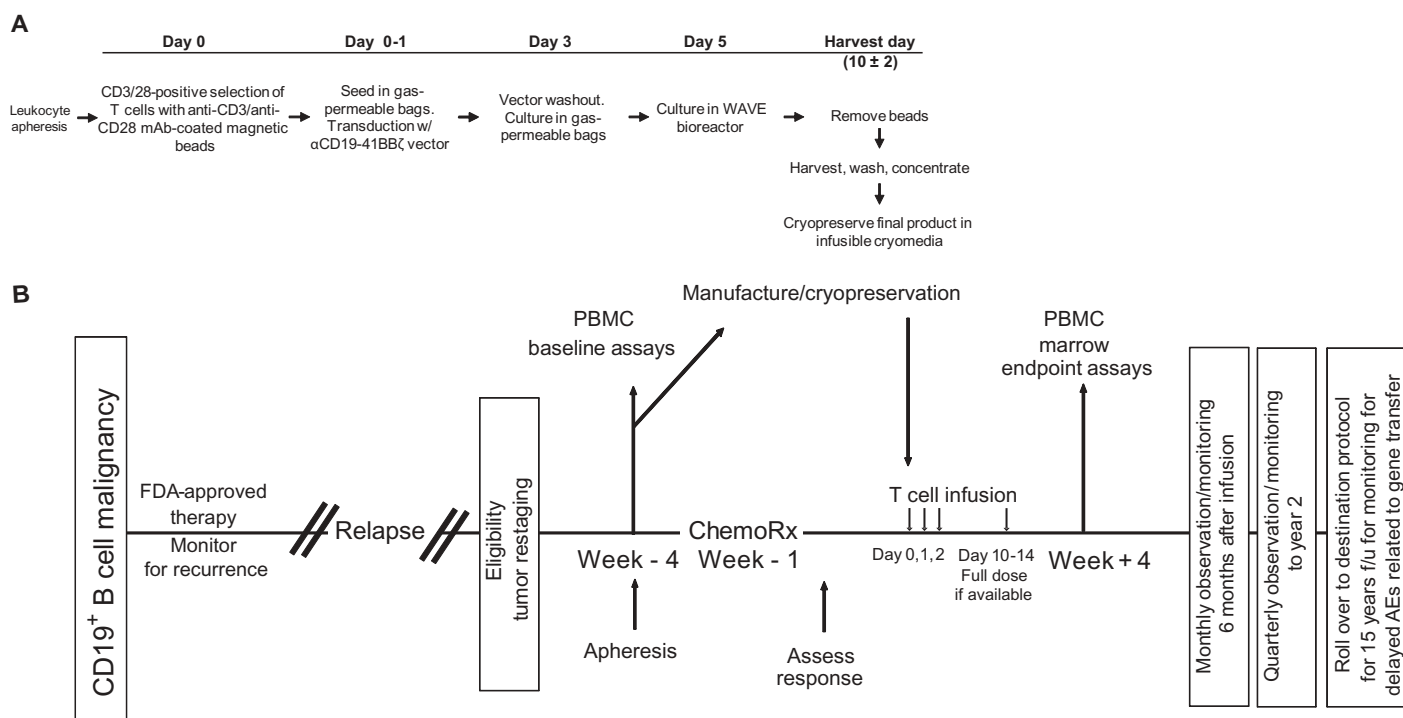
Fig. 1. Schematic representation of the gene transfer vector and transgene, gene-modified T cell manufacturing, and clinical protocol design. (**A**) T cell manufacturing. Autologous cells were obtained via leukapheresis, and T cells were enriched by mononuclear cell elutriation, washed, and expanded by addition of anti-CD3/CD28–coated paramagnetic beads for positive selection and activation of T cells. Residual leukemic cells were depleted. The lentiviral vector was added at the time of cell activation and was washed out on day 3 after culture initiation. Cells were expanded on a rocking platform device (WAVE Bioreactor System) for 8 to 12 days. On the final day of culture, the beads were removed by passage over a magnetic field and the CART19 cells were harvested and cryopreserved in infusible medium. mAb, monoclonal antibody. (**B**) Clinical protocol design. Patients were given lymphodepleting chemotherapy as described, followed by CART19 infusion #1 by intravenous gravity flow drip over a period of 15 to 20 min. The infusion was given using a split-dose approach over 3 days (10, 30, and 60%) beginning 1 to 5 days after completion of chemotherapy. Endpoint assays were conducted on study week 4. At the conclusion of active monitoring, subjects were transferred to a destination protocol for long-term follow-up as per FDA guidance.

publication is presented in tables S2 to S5. Of the analytes tested, 11 had a threefold or more change from baseline, including four cytokines [interleukin-6 (IL-6), interferon-γ (IFN-γ), IL-8, and IL-10], five chemokines [macrophage inflammatory protein–1α (MIP-1α), MIP-1β, monocyte chemotactic peptide–1 (MCP-1), CXC chemokine ligand 9 (CXCL9), and CXCL10], and the soluble receptors IL-1Rα

and IL-2Rα; IFN-γ had the largest relative change from baseline (Fig. 3). The peak time of cytokine elevation in UPN 01 and 03 correlated temporally with both the previously described clinical symptoms and the peak levels of CART19 cells detected in the blood for each patient. Notably, cytokine modulations were transient, and levels reverted to baseline relatively rapidly despite continued func-

Table 1. Patient demographics and response. CR, complete response; PR, partial response; N/A, not available.

Subject UPN	Age/sex karyotype	Previous therapies	CLL tumor burden at baseline			Total dose of CART19 (cells/kg)	Response day +30 (duration)
			BM (study day)‡	Blood (study day)‡	Nodes/spleen (study day)‡		
01	65/M normal	Fludarabine × four cycles (2002)	Hypercellular 70% CLL	N/A	6.2×10^{11} to 1.0×10^{12} CLL cells (day −37)	1.1×10^9 (1.6×10^7/kg)	CR (11+ months)
		Rituximab/fludarabine × four cycles (2005)	2.4×10^{12} CLL cells (day −14)				
		Alemtuzumab × 12 weeks (2006)	1.7×10^{12} CLL cells (day −1)				
		Rituximab (two courses, 2008 to 2009)					
		R-CVP × two cycles (2009)					
		Lenalidomide (2009)					
		PCR × two cycles (5/18/2010 to 6/18/2010)					
		Bendamustine × one cycle (7/31/10 to 8/1/10) pre-CART19					
02	77/M del (17)(p13)*	Alemtuzumab × 16 weeks (6/2007)	Hypercellular >95% CLL	2.75×10^{11} CLL cells (day −1)	1.2×10^{12} to 2.0×10^{12} CLL cells (day −24)	5.8×10^8 (1.0×10^7/kg)	PR (7 months)
		Alemtuzumab × 18 weeks (3/2009)	3.2×10^{12} CLL cells (day −47)				
		Bendamustine/rituximab:					
		7/1/2010 (cycle 1)					
		7/28/2010 (cycle 2)					
		8/26/2010 (cycle 3) pre-CART19					
03	64/M del (17)(p13)†	R-Fludarabine × two cycles (2002)	Hypercellular 40% CLL	N/A	3.3×10^{11} to 5.5×10^{11} CLL cells (day −10)	1.4×10^7 (1.46×10^5/kg)	CR (10+ months)
		R-Fludarabine × four cycles (10/06 to 1/07)	8.8×10^{11} CLL cells (day −1)				
		R-Bendamustine × one cycle (2/09)					
		Bendamustine × three cycles (3/09 to 5/09)					
		Alemtuzumab × 11 weeks (12/09 to 3/10)					
		Pentostatin/cyclophosphamide (9/10/10) pre-CART19					

*UPN 02 karyotype [International System for Human Cytogenetic Nomenclature (ISCN)]: 45,XY,del(1)(q25),+del(1)(p13),t(2;20)(p13;q11.2),t(3;5)(p13;q35),add(9)(p22),?del(13)(q14q34),−14,del(17)(p13)[cp24].   †UPN 03 karyotype (ISCN): 46,XY,del(17)(p12)[18]/44~46,idem,der(17)t(17;21)(p11.2;q11.2)[cp4]/40~45,XY,−17[cp3].   ‡See the Supplementary Material for methods of tumor burden determination.

tional persistence of CART19 cells. Only modest changes in cytokine levels were noted in UPN 02, possibly as a result of corticosteroid treatment. We also noted a robust induction of cytokine secretion in the supernatants from BM aspirates of UPN 03 (Fig. 3D and table S5). Although a pretreatment marrow sample was not available, compared to the late time point (+176), we also observed elevated levels for a number of factors in the +28 marrow sample for UPN 01 including IL-6, IL-8, IL-2R, and CXCL9; in contrast, compared to the pretreatment marrow sample, no elevation in cytokines was detected in the +31 day sample for UPN 02 (table S5).

One of the preclinical rationales for developing CAR$^+$ T cells with 4-1BB signaling domains was a projected reduced propensity to trigger IL-2 and tumor necrosis factor–α (TNF-α) secretion compared to CAR$^+$ T cells with CD28 signaling domains (7); indeed, elevated amounts of soluble IL-2 and TNF-α were not detected in the serum of the patients. Lower levels of these cytokines may be related to sustained clinical ac-

tivity: Previous studies have shown that CAR$^+$ T cells are potentially suppressed by regulatory T cells (13), which can be elicited by either CARs that secrete substantial amounts of IL-2 or by the provision of exogenous IL-2 after infusion. Moreover, the TNF-α is complicit in cytokine storm–related effects in patients, which are absent here.

Prolonged receptor expression and establishment of a population of memory CART19 cells in blood

A central question in CAR-mediated cancer immunotherapy is whether optimized cell manufacturing and costimulation domains will enhance the persistence of genetically modified T cells and permit the establishment of CAR$^+$ memory T cells in patients. Previous studies have not demonstrated robust expansion, prolonged persistence, or functional expression of CARs on T cells after infusion (14–17). The high persistence of CART19 cells that we observed at late time points for UPN 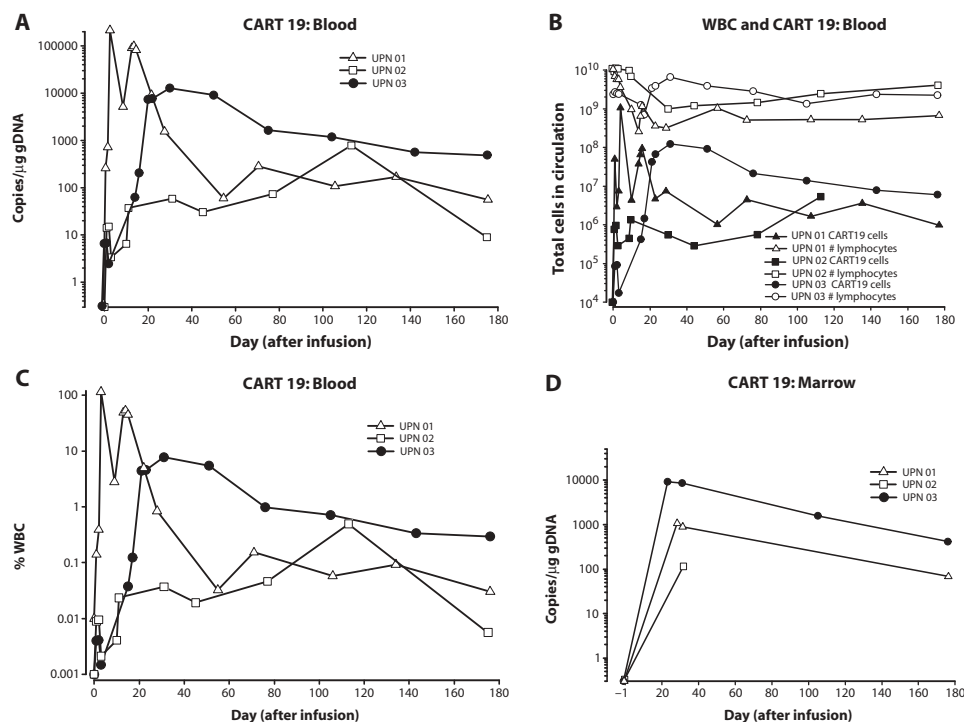03 facilitated a more detailed phenotypic analysis of persisting cells. Flow cytometric analysis of samples from both blood and BM 169 days after infusion revealed the presence of CAR19-expressing cells in UPN 03 as well as an absence of B cells (fig. S1, A and B). These CAR$^+$ cells persisted in all three patients beyond 4 months, as shown by qPCR (Fig. 2). The in vivo frequency of CAR$^+$ cells by flow cytometry closely matched the values obtained from the PCR assay for the CAR19 transgene. CAR expression was also detected on the surface of 5.7 and 1.7% of T cells in the blood of patient UPN 01 on days 71 and 286 after infusion (fig. S2).

We next used polychromatic flow cytometry to perform detailed studies and further characterize the expression, phenotype, and function of CART19 cells in UPN 03 using an anti-CAR idiotype antibody (MDA-647) and the gating strategy shown in fig. S3. We observed differences in the expression of memory and activation markers in both CD4$^+$ and CD8$^+$ T cells based on CAR19 expression.
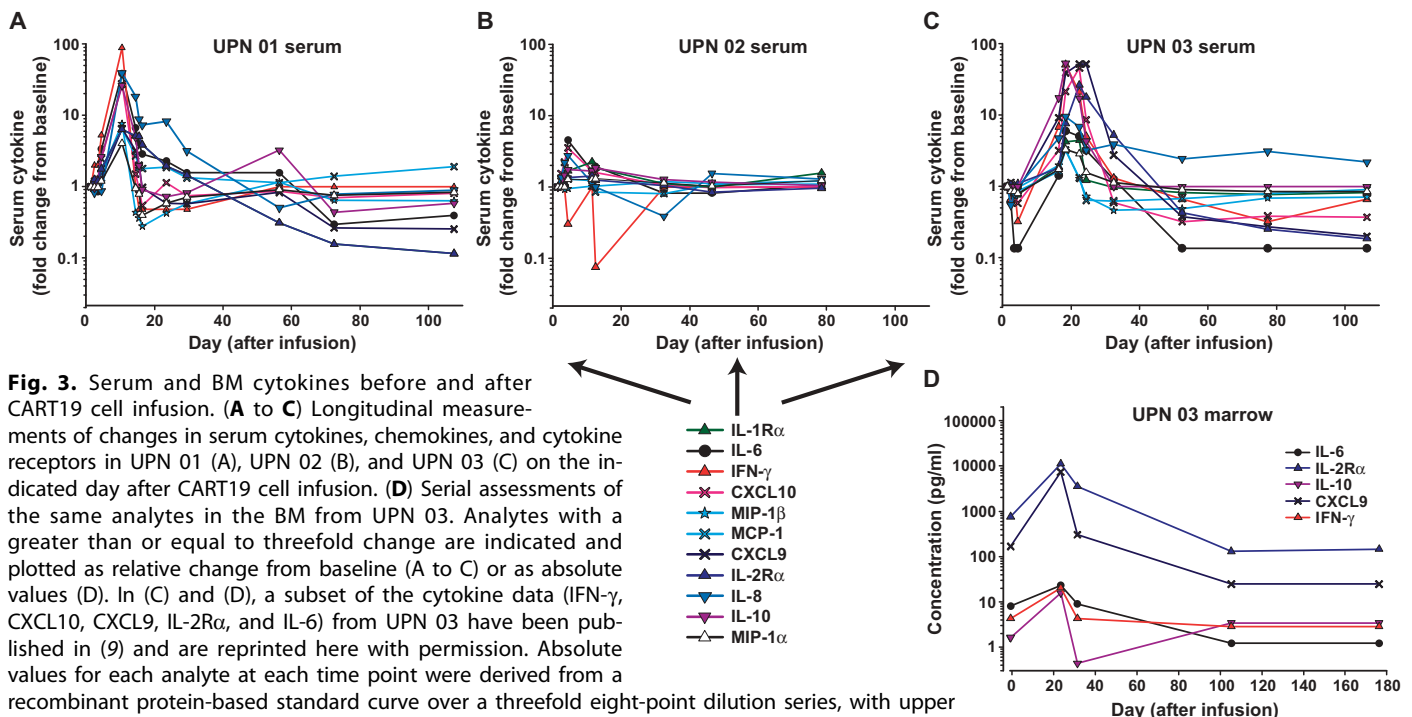
In the CD4$^+$ compartment, at day 56, CART19 cells were characterized by a uniform lack of CCR7, a predominance of CD27$^+$/CD28$^+$/PD-1$^+$ cells distributed within both CD57$^+$ and CD57$^-$ compartments, and an essential absence of CD25 and CD127 expression, the latter two markers defining regulatory CD4$^+$ T cells (18) (Fig. 4A). In contrast, CAR$^-$ cells at this time point were heterogeneous in CCR7, CD27, and PD-1 expression; expressed CD127; and also contained a substantial CD25$^+$/CD127$^-$ population. By day 169, although CD28 expression remained uniformly positive in all CART19 CD4$^+$ cells, a fraction of the CART19 CD4$^+$ cells had acquired a central memory phenotype, with

Fig. 2. Sustained in vivo expansion and persistence in blood and marrow of CART19 cells. (**A** to **D**) qPCR analysis was performed on DNA isolated from whole blood (A to C) or bone marrow (BM) (D) samples obtained from UPN 01, UPN 02, and UPN 03 to detect and quantify CAR19 sequences. The frequency of CART19 cells is shown as average transgene copies (A), total calculated CART19 cells in circulation (B), or as a fraction of circulating white blood cells (WBCs) (C). (A) Copies CAR19/microgram DNA is calculated as described in Materials and Methods. (B) The total number of lymphocytes (total normal and CLL cells) versus total CART19$^+$ cells in circulation is plotted for all three subjects using the absolute lymphocyte count from complete blood count values and assuming a 5.0-liter volume of peripheral blood. (C) % WBC is calculated as described in Materials and Methods. (D) Bulk qPCR analysis of marrow to quantify CART19 sequences. The data from patient UPN 03 in (A, C, and D) has been published in (9) and is reprinted here with permission. Each data point represents the average of triplicate measurements on 100 to 200 ng of genomic DNA, with maximal percent coefficient of variation (CV) less than 1.56%. Pass/fail parameters for the assay included preestablished ranges for slope and efficiency of amplification, and amplification of a reference sample. The lower limit of quantification for the assay established by the standard curve range was two copies of transgene per microgram of genomic DNA; sample values below that number are considered estimates and presented if at least two of three replicates generated a C_t value with percent CV for the values 15%. CART19 cells were infused at days 0, 1, and 2 for UPN 01 and 03 and at days 0, 1, 2, and 11 for UPN 02.

CCR7 expression, a higher percentage of CD27⁻ cells, the appearance of a PD-1⁻ subset, and acquisition of CD127 expression. At day 169, CAR⁻ cells remained reasonably consistent with their day 56 counterparts, with the exception of a reduction in CD27 expression and a decrease in the percentage of CD25⁺/CD127⁻ cells.

In the CD8⁺ compartment, at day 56, CART19 CD8⁺ cells displayed primarily an effector memory phenotype (CCR7⁻, CD27⁻, CD28⁻), consistent with prolonged and robust exposure to antigen (Fig. 4B). In contrast, CAR⁻ CD8⁺ T cells consisted of mixtures of effector and central memory cells, with CCR7 expression in a subset of cells, and substantial numbers of cells in the CD27⁺/CD28⁻ and CD27⁺/CD28⁺ fractions. Although a large percentage of both CART19 and CAR⁻ cell populations expressed CD57, a marker associated with memory T cells with high cytolytic potential (19), this molecule was uniformly coexpressed with PD-1 in the CART19 cells, a possible reflection of the extensive replicative history of these cells. In contrast to the CAR⁻ cell population, the entirety of the CART19 CD8⁺ population lacked expression of both CD25 and CD127, markers associated with T cell activation and the development of functional memory cells (20). By day 169, although the phenotype of the CAR⁻ cell population remained similar to the day 56 cells, the CART19 population had evolved to contain a population with features of central memory cells, notably expression of CCR7 and higher levels of CD27 and CD28, as well as cells that were PD-1⁻, CD57⁻, and CD127⁺.

Effector function of CART19 cells after 6 months in blood

In addition to a lack of long-term persistence, a limitation of previous trials with CAR⁺ T cells has been the rapid loss of functional activity of the infused T cells in vivo. The high level of CART19 cell persistence and surface expression of the CAR19 molecule in UPN 03 provided the opportunity to directly test anti-CD19–specific effector functions in cells recovered from cryopreserved PB samples. Peripheral blood mononuclear cells (PBMCs) from UPN 03 were cultured with target cells that either did or did not express CD19 (Fig. 4C and fig. S3). Robust CD19-specific effector function of CART19 cells was observed by the specific degranulation of CART19 cells against CD19⁺ but not CD19⁻ target cells, as assessed by surface CD107a expression. Notably, exposure of the CART19 population to CD19⁺ targets induced a rapid internalization of surface CAR19 (see fig. S3 for constitutive surface expression of CAR19 in the same effector cells in standard flow cytometric staining). The presence of costimulatory molecules on target cells was not required for triggering CART19 cell degranulation because the NALM-6 line, which was used as a target in these studies, does not express CD80 or CD86 (21). Effector function was evident at day 56 after infusion and was retained at day 169 (Fig. 4C). Robust effector function of CAR⁺ and CAR⁻ T cells could also be demonstrated by pharmacologic stimulation with phorbol 12-myristate 13-acetate (PMA) and ionomycin.

Fig. 3. Serum and BM cytokines before and after CART19 cell infusion. (**A** to **C**) Longitudinal measurements of changes in serum cytokines, chemokines, and cytokine receptors in UPN 01 (A), UPN 02 (B), and UPN 03 (C) on the indicated day after CART19 cell infusion. (**D**) Serial assessments of the same analytes in the BM from UPN 03. Analytes with a greater than or equal to threefold change are indicated and plotted as relative change from baseline (A to C) or as absolute values (D). In (C) and (D), a subset of the cytokine data (IFN-γ, CXCL10, CXCL9, IL-2Rα, and IL-6) from UPN 03 have been published in (9) and are reprinted here with permission. Absolute values for each analyte at each time point were derived from a recombinant protein-based standard curve over a threefold eight-point dilution series, with upper and lower limits of quantification determined by the 80 to 120% observed/expected cutoff values for the standard curves. Each sample was evaluated in duplicate with average values calculated and percent CV in most cases less than 10%. To accommodate consolidated data presentation in the context of the wide range for the absolute values, data are presented as fold change over the baseline value for each analyte. In cases where baseline values were not detectable, half of the lowest standard curve value was used as the baseline value. Standard curve ranges for analytes and baseline (day 0) values (listed in parentheses sequentially for UPN 01, 02, and 03), all in pg/ml: IL-1Rα: 35.5 to 29,318 (689, 301, and 287); IL-6: 2.7 to 4572 (7, 10.1, and 8.7); IFN-γ: 11.2 to 23,972 (2.8, not detected, and 4.2); CXCL10: 2.1 to 5319 (481, 115, and 287); MIP-1β: 3.3 to 7233 (99.7, 371, and 174); MCP-1: 4.8 to 3600 (403, 560, and 828); CXCL9: 48.2 to 3700 (1412, 126, and 177); IL-2Rα: 13.4 to 34,210 (4319, 9477, and 610); IL-8: 2.4 to 5278 (15.3, 14.5, and 14.6); IL-10: 6.7 to 13,874 (8.5, 5.4, and 0.7); MIP-1α: 7.1 to 13,778 (57.6, 57.3, and 48.1).

Profound antitumor clinical activity of CART19 cells

There were no significant toxicities observed during the 4 days after the infusion in any patient other than transient febrile reactions. However, all patients subsequently developed significant clinical and laboratory toxicities between days 7 and 21 after the first infusion. With the exception of B cell aplasia, these toxicities were short-term and reversible. Of the three patients treated to date, there are two complete responses and one partial response lasting greater than 8 months after CART19 infusion according to standard criteria (22). Details of past medical history and response to therapy are described in Table 1. The clinical course of UPN 03 has been described in detail (9).

In brief, patient UPN 02 was treated with two cycles of bendamustine with rituximab, resulting in stable disease; he received a third dose of bendamustine as lymphodepleting chemotherapy before CART19 cell infusion. After CART19 infusion, and coincident with the onset of high fevers, he had rapid clearance of the p53-deficient CLL cells

from his PB (Fig. 5A) and a partial reduction of adenopathy. He developed fevers to 40°C, rigors, and dyspnea requiring a 24-hour hospitalization on day 11 after the first infusion and on the day of his second CART19 cell boost. Fevers and constitutional symptoms persisted, and on day 15, he had transient cardiac dysfunction; all symptoms resolved after corticosteroid therapy was initiated on day 18. His BM showed persistent extensive infiltration of CLL 1 month after therapy despite marked PB cytoreduction. He remained asymptomatic at the time of publication.

Patient UPN 01 developed a febrile syndrome, with rigors and transient hypotension beginning 10 days after infusion. The fevers persisted for about 2 weeks and resolved; he has had no further constitutional symptoms. He achieved a rapid and complete response (Fig. 5, B and C). Between 1 and 6 months after infusion, no circulating CLL cells were detected in the blood by deep sequencing (Table 2). His BM at 1, 3, and 6 months after CART19 cell infusions showed sustained
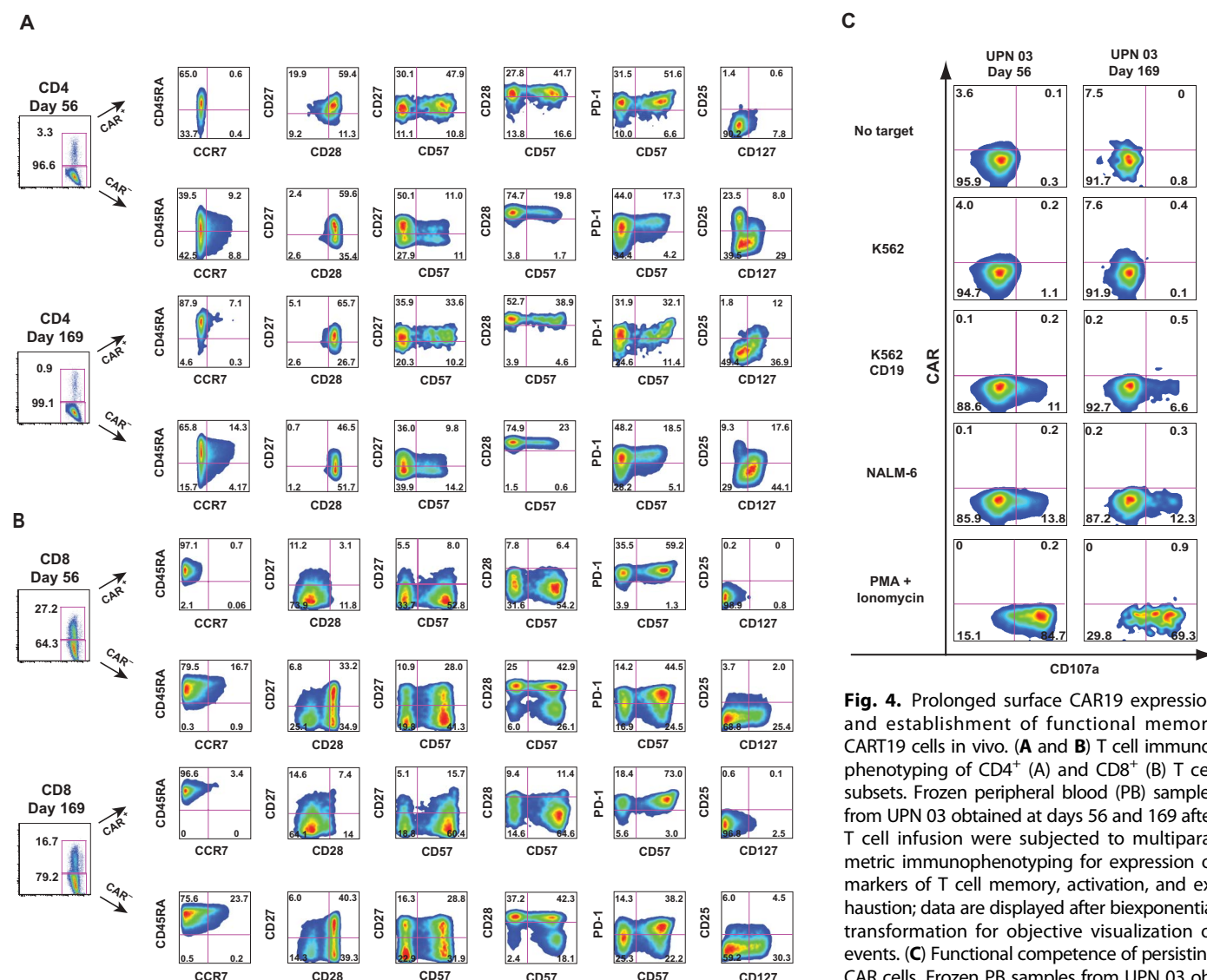

Fig. 4. Prolonged surface CAR19 expression and establishment of functional memory CART19 cells in vivo. (**A** and **B**) T cell immunophenotyping of CD4^{+} (A) and CD8^{+} (B) T cell subsets. Frozen peripheral blood (PB) samples from UPN 03 obtained at days 56 and 169 after T cell infusion were subjected to multiparametric immunophenotyping for expression of markers of T cell memory, activation, and exhaustion; data are displayed after biexponential transformation for objective visualization of events. (**C**) Functional competence of persisting CAR cells. Frozen PB samples from UPN 03 obtained at days 56 and 169 after T cell infusion were evaluated directly ex vivo for the ability to recognize CD19-expressing target cells using CD107 degranulation assays. Presented data are for the CD8^{+} gated population. The gating strategies for these figures are presented in fig. S2.

absence of the lymphocytic infiltrate by morphology and immuno-histochemical analysis (Fig. 5B). Computed tomography (CT) scans at 1 and 3 months after infusion showed resolution of adenopathy (Fig. 5C). His complete remission was sustained for more than 10 months at the time of this report.

Molecular elimination of tumor and normal B cell reconstitution in patients

Using high-throughput immunoglobulin H (IgH) immune profiling, we characterized the tumor burdens and normal B cell mass in patients UPN 01 and 03 (Table 2). For both patients, we evaluated the complete B cell repertoire in patient PB samples obtained before enrollment, at day −1 before T cell infusion, and after treatment in PB- and BM-derived samples by quantifying rearranged CDR3 domains in IGH@ loci via deep sequencing; we did not evaluate material from UPN 02 because he had clinically documented disease after corticosteroid administration and residual $CD19^+CD20^+$ cells detected by clinical laboratory analysis. In both patients, the preenrollment samples were dominated by the presence of a single patient-unique CLL clone (99.7% in UPN 01 and 90.4% in UPN 03). No reduction in tumor clone frequency was observed in UPN 01 (clone frequency, 99.8%) and UPN 03 (88.9%) after the preinfusion conditioning regimen. No rearranged B cell sequences were detected for either UPN 01 and 03 samples at the first time points after infusion (days 28 and 31, respectively) in either PB or BM samples. At the day +176 time point, normal rearranged B cell sequences could be detected in both PB (7362 of 285,305 sequences) and BM samples (4451 of 202,535 sequences) for UPN 01, consistent with reconstitution of normal B cells. No rearranged B cell sequences could be detected at this time point in PB or BM for UPN 03. Notably, no rearranged IGH@ sequences related to the original tumor could be detected in the day +176 PB or BM for either UPN 01 (PB: 0 of 285,305 sequence reads, BM: 0 of 202,305 sequence reads) or UPN 03 (PB: 0 of 317,460, BM: 0 of 158,730 reads).

Plasma cells resident in the BM may be targets of CART19 cells

Plasma cells were enumerated in the BM of the patients by CD138 immunohisto-chemistry on the core biopsies (table S9). In UPN 01, no $CD138^+$ cells were identified after infusion, whereas in UPN 02 and UPN 03, residual $CD138^+$ cells were present after infusion, at lower levels than in the preinfusion BMs. These results are consistent with reports that most normal human plasma cells express CD19, unlike myeloma cells (23, 24). Consistent with this, the serum immunoglobulin levels declined in UPN 01 (table S10) and in UPN 03 (9).

Considerations of in vivo CART19 effector–to–CLL target cell ratio

In our preclinical studies, we found that large tumors could be ablated and that the infusion of 2.2×10^7 CAR T cells could eradicate tumors composed of 1×10^9 cells, for an in vivo effector-to-target (E/T) ratio of 1:42 in humanized mice (8), although these calculations did not take into account the expansion of T cells after injection. Estimation of CLL tumor burden over time permitted the calculation of tumor reduction and the estimated CART19 E/T ratios achieved in vivo in the three subjects based on number of CAR^+ T cells infused. Tumor burdens were calculated by measuring CLL load in BM, blood, and secondary lymphoid tissues as described in the Supplementary Material. The baseline tumor burdens (Table 1) indicate that each patient had on the order of 10^{12} CLL cells (that is, about 1 kg of tumor load) before CART19 infusion (tables S7 and S8). Patient UPN 03 had an estimated baseline tumor burden of 8.8×10^{11} CLL cells in the BM on day −1 (after chemotherapy and before CART19 infusion) and a measured tumor mass in secondary lymphoid tissues of 3.3 to 5.5×10^{11} CLL cells. UPN 03 was infused with only 1.4×10^7 CART19 cells;
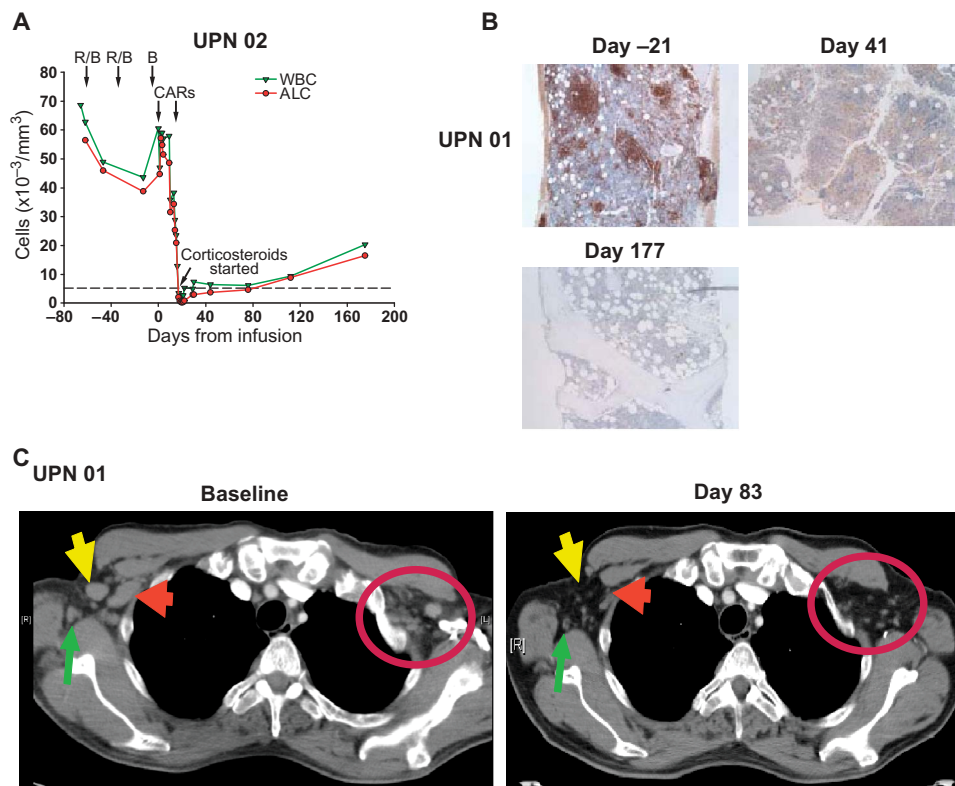

Fig. 5. Evaluation of clinical responses after infusion of CART19 cells. (**A**) UPN 02 was treated with two cycles of rituximab and bendamustine with minimal response (R/B, arrows). CART19 cells were infused beginning 4 and 14 days after bendamustine only (B, arrow). The rituximab- and bendamustine-resistant leukemia was rapidly cleared from blood, as indicated by a decrease in the absolute lymphocyte count (ALC) from 60,600/μl to 200/μl within 18 days of the infusion. Corticosteroid treatment was started on day 18 after infusion because of malaise and noninfectious febrile syndrome. The reference line (dotted) indicates the upper normal limit for ALC. (**B**) Sequential BM biopsy or clot specimens from UPN 01 were stained for CD20. Leukemia infiltration was present before treatment was absent after treatment; normalization of cellularity and trilineage hematopoiesis were also observed. (**C**) Sequential CT imaging indicates rapid resolution of chemotherapy-resistant generalized lymphadenopathy. Bilateral axillary masses in UPN 01 resolved by 83 days after infusion, as indicated by arrows and circle.

Table 2. High-resolution characterization of residual tumor burden and normal B cells in UPN 01 and 03. Analyses were performed on DNA isolated from whole blood by high-throughput IgH immune profiling (Adaptive TcR Corp.). PB, peripheral blood; BM, bone marrow.

Patient (UPN)	Tissue	Time point	Amount of DNA in PCR (ng)	Cell equivalents	Total productive sequence reads	Total productive unique B cell clonotypes	CLL *IGH@* CDR3 clone reads	Clone frequency (% productives)
01	PB	Pre-infusion	1000	158,730	184,786	24	184,256	99.713
01	PB	Day −1	1000	158,730	408,579	48	407,592	99.758
01	PB	Day +28	1000	158,730	0	0	0	0.000
01	PB	Day +176	500	79,365	285,305	7,362	0	0.000
01	BM	Day +28	1000	158,730	0	0	0	0.000
01	BM	Day +176	1000	158,730	202,535	4,451	0	0.000
03	PB	Pre-infusion	2000	317,460	22,074,912	58,234	19,948,508	90.367
03	PB	Day −1	386	61,270	1,385,340	4,544	1,231,018	88.860
03	PB	Day +31	1000	158,730	0	0	0	0.000
03	PB	Day +176	2000	317,460	0	0	0	0.000
03	BM	Day +31	1750	277,778	0	0	0	0.000
03	BM	Day +176	1000	158,730	0	0	0	0.000

using the estimate of initial total tumor burden (1.3×10^{12} CLL cells) and the observation that no CLL cells were detectable after treatment, we achieved a marked 1:93,000 E/T ratio. By similar calculations, an effective E/T ratio in vivo of 1:2200 and 1:1000 was calculated for UPN 01 and 02 (table S6). Therefore, a contribution of serial killing by CART19 cells combined with in vivo CART19 expansion of >1000-fold likely contributed to the powerful antileukemic effects mediated by CART19 cells.

DISCUSSION

Insufficient persistence, expression, and effector function of CARs in vivo has resulted in limited success in the trials testing first-generation CAR T cells (14–16, 25, 26). Because preclinical modeling demonstrated enhanced persistence of CARs that incorporated a 4-1BB signaling molecule (7, 8), we developed second-generation CARs engineered with lentiviral vector technology—an approach that was previously found to be safe in the setting of chronic HIV infection (27). Our results show that when second-generation CARs were expressed in T cells and cultured under conditions designed to promote engraftment of central memory T cells (28, 29), CAR+ T cell expansion after infusion was improved compared to previous reports. Moreover, CART19 cells induced a CD19-specific cellular memory response. These CART19 cells tracked efficiently to sites of tumor and became established as de facto "tumor-infiltrating lymphocytes" that exhibited CD19 specificity and retained effector function in vivo in patient blood and marrow specimens for months.

What drives the expansion and persistence of CART19 cells in vivo? Our study is one of few trials to have omitted IL-2 infusions (17, 26); thus, the CART19 cells likely expanded in response either to

homeostatic cytokines or to CD19 expressed on leukemic targets and/or normal B cells. Indeed, the kinetics of cytokine release in serum and BM after the introduction of CART19 into patients correlated with peak CART19 numbers, which suggests that the decline in CART19 numbers may be initiated when cellular targets expressing CD19 become limiting. The extended survival of these cells may be due in part to the incorporation of the 4-1BB domain into the CAR itself or because of signaling through either the natural T cell receptor (TCR) or CAR. Another possibility is related to the presence of CART19 cells in BM specimens: CART19 cells could be maintained by encountering B cell progenitors in the BM. This potential stimulation of CART19 cells by normal B cells may provide a mechanism for CAR memory by means of "self-vaccination/boosting" and, therefore, long-term tumor immunosurveillance. Although the mechanisms driving CART19 homeostasis remain unclear, CAR therapy is clearly not always a transient form of immunotherapy, as has been previously supposed. Thus, CARs with optimized signaling domains may have a role both in remission induction and consolidation and in continued immunosurveillance in cancer patients.

Our studies indicate that persisting CART19 cells consist of both central and effector memory T cells, which likely contributes to their long-term survival compared to previous reports. Signaling of 4-1BB has been reported to promote the development of memory in the context of TCR signaling (30). But whether CAR T cells can differentiate in vivo into a central memory–like state upon encounter and subsequent elimination of target cells expressing the surrogate antigen remains to be resolved.

We have observed potent antileukemic effects in all three patients examined (9), including two patients with p53-deficient leukemia. Previous studies with CARs have had difficulty separating antitumor effects from lymphodepleting chemotherapy. However, the delayed cytokine release, combined with the kinetics of tumor lysis in fludarabine-refractory

patients that was coincident, and possibly dependent, on in vivo CAR expansion in our study, indicates that CART19 cells mediate potent antitumor effects. The present results do not exclude a role for chemotherapy in potentiating the effects of CARs, and a number of studies suggest plausible mechanisms for coordinate effects of chemotherapy and CAR T cells (31, 32) in addition to the lymphodepleting aspects of chemotherapy, which promotes homeostatic expansion of T cells (33), including, presumably, CART19 cells.

We have found that very low doses of CARs can elicit potent clinical responses. However, the results to date do not support an obvious dose-response relationship. This pilot study was not designed to determine optimal biologic dose with what is essentially a dynamic cell product, but to demonstrate safety of the CAR19 vector design. Nonetheless, the observation that doses of CART19 cells several orders of magnitude below those tested in previous trials can have clinical benefit may have important implications for future implementation of CAR therapy on a wider scale as well as for the design of trials testing CARs directed against targets other than CD19.

Although our second-generation CAR T cells led to considerable clinical effects, the lysis of at least a kilogram of tumor burden in all three patients was accompanied with the delayed release of potentially dangerously high levels of cytokines in two of the patients (9). We did not observe classical cytokine storm effects; however, our trial was designed to mitigate this possibility by deliberate infusion of CART19 cells over a period of 3 days and by using signaling domains that did not promote secretion of IL-2 and TNF-α.

Humoral and cellular immunity against CAR-modified T cells has been reported in other studies (34, 35). The presence of cells that express surface CAR19 at 6 and 9 months after T cell infusion strongly suggests the absence of cellular and humoral immune responses against CART19 cells. The absence of antibody responses is not surprising because the therapy effectively eliminated B cells in patients. On the other hand, the absence of cellular immunity against CART19 cells is perhaps surprising because the CAR19 construct contains both murine sequences (the antibody determinants) and unique junctional fragments between the different components of the CAR19 construct. These results raise the possibility that B cell help may be required to prime T cell responses. It remains to be determined whether the severe immunosuppression at baseline in the heavily pretreated CLL patients might have contributed to the inability to reject the CART19 cells.

We used lentivirus vectors to transfer CAR19 into patient T cells. Lentiviral vectors have the potential to be safer than retroviruses from the perspective of insertional mutagenesis, and they have substantially higher efficiency for genetically engineering human T cells (36, 37). We conducted the first study using a lentiviral vector for gene transfer in HIV (27). In that study, and in patients enrolled in subsequent lentiviral vector–engineered T cells studies (clinicaltrials.gov NCT00295477 and NCT00622232), no adverse events related to gene transfer have been observed in more than 280 patient-years of observation. Analysis of vector integration sites in several of these patients has not revealed any evidence for abnormal expansions of cells due to vector-mediated insertional activation of proto-oncogenes (38). Nonetheless, it will be important to continue to monitor patients enrolled in this and other lentiviral gene transfer clinical trials carefully, particularly when new constructs or targets are tested.

A thorough comparison of the vector, transgene, and cell manufacturing procedures with results from ongoing studies at other centers will be required to gain a full understanding of the key features required to obtain sustained function of CAR-expressing T cells in vivo. Unlike antibody therapies, CAR-modified T cells have the potential to replicate in vivo, and long-term persistence could lead to sustained tumor control and obviate the need for repeated infusions of antibody. The availability of an off-the-shelf therapy composed of non–cross-resistant killer T cells has the potential to improve the outcome of patients with B cell malignancies.

MATERIALS AND METHODS

General laboratory statement
Research sample processing, freezing, and laboratory analyses were performed in the Translational and Correlative Studies Laboratory (TCSL) at the University of Pennsylvania, which operates under principles of Good Laboratory Practice with established standard operating procedures and/or protocols for sample receipt, processing, freezing, and analysis. Assay performance and data reporting conform to MIATA guidelines (39).

Protocol design
The clinical trial (NCT01029366) was conducted as diagrammed in Fig. 1. Patients with CD19$^+$ hematologic malignancy with persistent disease after at least two previous treatment regimens and who were not eligible for allogeneic stem cell transplantation were eligible. After tumor restaging, PB T cells for CART19 manufacturing were collected by apheresis and the subjects were given a single course of chemotherapy during the week before infusion, as specified in Table 1. CART19 cells were administered by intravenous infusion with a 3-day split-dose regimen (10, 30, and 60%) at the dose indicated in Table 1, and, if available, a second dose was administered on day 10; only UPN 02 had sufficient cells for a second infusion. Subjects were assessed for toxicity and response at frequent intervals for at least 6 months. The protocol was approved by the U.S. Food and Drug Administration (FDA), the Recombinant DNA Advisory Committee, and the Institutional Review Board of the University of Pennsylvania. The first day of infusion was set as study day 0.

Subjects: Clinical summary
The clinical summaries are outlined in Table 1. UPN 01 was first diagnosed with stage II B cell CLL at age 55 in November 2000. He was asymptomatic and observed for about 1.5 years until he required therapy for progressive lymphocytosis, thrombocytopenia, adenopathy, and splenomegaly in February 2002. Over the course of the next 8 years, he received prior lines of therapy. His most recent therapy was two cycles of pentostatin, cyclophosphamide, and rituximab 2 months before CART19 cell infusion—with a minimal response. He then received one cycle of bendamustine as lymphodepleting chemotherapy before CART19 cell infusion.

UPN 02 was first diagnosed with CLL in 2000 at age 68 when he presented with fatigue and leukocytosis. He was relatively stable for 4 years, when he developed progressive leukocytosis (195,000/μl), anemia, and thrombocytopenia requiring therapy. Karyotypic analysis showed that the CLL cells had a deletion of chromosome 17p. Because of progressive disease in 2007, he was treated with alemtuzumab with a partial response, but within 1.5 years, he had progressive disease. He was re-treated with alemtuzumab for 18 weeks with a partial response and a 1-year progression-free interval. He then received two cycles of

bendamustine with rituximab without a significant response (Fig. 5A). He received single-agent bendamustine as lymphodepleting chemotherapy before CART19 cell infusion.

The clinical summary of UPN 03 is as previously described (*9*).

Vector production

The CD19-BB-z transgene (GeMCRIS 0607-793) was designed and constructed as described (*7*). A lentiviral vector was produced according to current good manufacturing practices with a three-plasmid production approach at Lentigen Corp., as described (*40*).

Preparation of CART19 cell product

Methods of T cell preparation with paramagnetic polystyrene beads coated with anti-CD3 and anti-CD28 monoclonal antibodies have been described (*41*). Lentiviral transduction was performed as described (*27*).

Measurement of transgene persistence in vivo

Refer to the Supplementary Material.

Soluble factor analysis

Refer to the Supplementary Material for quantification of soluble factors and cytokines in serum and BM.

Multiparameter flow cytometry

Refer to the Supplementary Material.

Cellular assays

Refer to the Supplementary Material.

SUPPLEMENTARY MATERIAL

www.sciencetranslationalmedicine.org/cgi/content/full/3/95/95ra73/DC1
Methods
Fig. S1. Prolonged surface CART19 expression and absent B cells in vivo in blood and marrow of UPN 03.
Fig. S2. Direct ex vivo detection of CART19-positive cells in UPN 01 PBMC 71 and 286 days after T cell infusion.
Fig. S3. Gating strategy to identify CART19 expression using polychromatic flow cytometry in UPN 03 blood specimens.
Table S1. Apheresis products and CART19 product release criteria.
Table S2. Longitudinal measurement of absolute levels for circulating cytokines/chemokines/growth factors in serum from patient UPN 01.
Table S3. Longitudinal measurement of absolute levels for circulating cytokines/chemokines/growth factors in serum from patient UPN 02.
Table S4. Longitudinal measurement of absolute levels for circulating cytokines/chemokines/growth factors in serum from patient UPN 03.
Table S5. Longitudinal measurement of absolute levels for marrow cytokines, chemokines, and growth factors in serum obtained from bone marrow samples from patients UPN 01, UPN 02, and UPN 03.
Table S6. Calculated CART19 effector/target ratios achieved in vivo.
Table S7. Percentage and mass of CLL in active bone marrow.
Table S8. Patient tumor volume in secondary lymphoid tissues.
Table S9. Bone marrow plasma cell percentages in patients UPN 01, UPN 02, and UPN 03.
Table S10. Serum immunoglobulin levels in UPN 01.
References

REFERENCES AND NOTES

1. G. Gross, T. Waks, Z. Eshhar, Expression of immunoglobulin-T-cell receptor chimeric molecules as functional receptors with antibody-type specificity. *Proc. Natl. Acad. Sci. U.S.A.* **86**, 10024–10028 (1989).
2. B. A. Irving, A. Weiss, The cytoplasmic domain of the T cell receptor ζ chain is sufficient to couple to receptor-associated signal transduction pathways. *Cell* **64**, 891–901 (1991).
3. D. B. Kohn, G. Dotti, R. Brentjens, B. Savoldo, M. Jensen, L. J. Cooper, C. H. June, S. Rosenberg, M. Sadelain, H. E. Heslop, CARS on track in the clinic. *Mol. Ther.* **19**, 432–438 (2011).
4. B. Jena, G. Dotti, L. J. Cooper, Redirecting T-cell specificity by introducing a tumor-specific chimeric antigen receptor. *Blood* **116**, 1035–1044 (2010).
5. F. M. Uckun, W. Jaszcz, J. L. Ambrus, A. S. Fauci, K. Gajl-Peczalska, C. W. Song, M. R. Wick, D. E. Myers, K. Waddick, J. A. Ledbetter, Detailed studies on expression and function of CD19 surface determinant by using B43 monoclonal antibody and the clinical potential of anti-CD19 immunotoxins. *Blood* **71**, 13–29 (1988).
6. M. Sadelain, R. Brentjens, I. Rivière, The promise and potential pitfalls of chimeric antigen receptors. *Curr. Opin. Immunol.* **21**, 215–223 (2009).
7. M. C. Milone, J. D. Fish, C. Carpenito, R. G. Carroll, G. K. Binder, D. Teachey, M. Samanta, M. Lakhal, B. Gloss, G. Danet-Desnoyers, D. Campana, J. L. Riley, S. A. Grupp, C. H. June, Chimeric receptors containing CD137 signal transduction domains mediate enhanced survival of T cells and increased antileukemic efficacy in vivo. *Mol. Ther.* **17**, 1453–1464 (2009).
8. C. Carpenito, M. C. Milone, R. Hassan, J. C. Simonet, M. Lakhal, M. M. Suhoski, A. Varela-Rohena, K. M. Haines, D. F. Heitjan, S. M. Albelda, R. G. Carroll, J. L. Riley, I. Pastan, C. H. June, Control of large, established tumor xenografts with genetically retargeted human T cells containing CD28 and CD137 domains. *Proc. Natl. Acad. Sci. U.S.A.* **106**, 3360–3365 (2009).
9. D. L. Porter, B. L. Levine, M. Kalos, A. Bagg, C. H. June, Chimeric antigen receptor-modified T cells in chronic lymphoid leukemia. *N. Engl. J. Med.*, 10.1056/NEJMoa1103849 (2011).
10. H. Döhner, K. Fischer, M. Bentz, K. Hansen, A. Benner, G. Cabot, D. Diehl, R. Schlenk, J. Coy, S. Stilgenbauer, M. Volkmann, P. R. Galle, A. Poustka, W. Hunstein, P. Lichter, p53 gene deletion predicts for poor survival and non-response to therapy with purine analogs in chronic B-cell leukemias. *Blood* **85**, 1580–1589 (1995).
11. A. G. Ramsay, A. J. Johnson, A. M. Lee, G. Gorgün, R. Le Dieu, W. Blum, J. C. Byrd, J. G. Gribben, Chronic lymphocytic leukemia T cells show impaired immunological synapse formation that can be reversed with an immunomodulating drug. *J. Clin. Invest.* **118**, 2427–2437 (2008).
12. B. L. Levine, W. B. Bernstein, M. Connors, N. Craighead, T. Lindsten, C. B. Thompson, C. H. June, Effects of CD28 costimulation on long-term proliferation of CD4⁺ T cells in the absence of exogenous feeder cells. *J. Immunol.* **159**, 5921–5930 (1997).
13. J. C. Lee, E. Hayman, H. J. Pegram, E. Santos, G. Heller, M. Sadelain, R. Brentjens, In vivo inhibition of human CD19-targeted effector T cells by natural T regulatory cells in a xenotransplant murine model of B cell malignancy. *Cancer Res.* **71**, 2871–2881 (2011).
14. M. H. Kershaw, J. A. Westwood, L. L. Parker, G. Wang, Z. Eshhar, S. A. Mavroukakis, D. E. White, J. R. Wunderlich, S. Canevari, L. Rogers-Freezer, C. C. Chen, J. C. Yang, S. A. Rosenberg, P. Hwu, A phase I study on adoptive immunotherapy using gene-modified T cells for ovarian cancer. *Clin. Cancer Res.* **12**, 6106–6115 (2006).
15. C. H. Lamers, R. Sleijfer, A. G. Vulto, W. H. Kruit, M. Kliffen, R. Debets, J. W. Gratama, G. Stoter, E. Oosterwijk, Treatment of metastatic renal cell carcinoma with autologous T-lymphocytes genetically retargeted against carbonic anhydrase IX: First clinical experience. *J. Clin. Oncol.* **24**, e20–e22 (2006).
16. B. G. Till, M. C. Jensen, J. Wang, E. Y. Chen, B. L. Wood, H. A. Greisman, X. Qian, S. E. James, A. Raubitschek, S. J. Forman, A. K. Gopal, J. M. Pagel, C. G. Lindgren, P. D. Greenberg, S. R. Riddell, O. W. Press, Adoptive immunotherapy for indolent non-Hodgkin lymphoma and mantle cell lymphoma using genetically modified autologous CD20-specific T cells. *Blood* **112**, 2261–2271 (2008).
17. B. Savoldo, C. A. Ramos, E. Liu, M. P. Mims, M. J. Keating, G. Carrum, R. T. Kamble, C. M. Bollard, A. P. Gee, Z. Mei, H. Liu, B. Grilley, C. M. Rooney, H. E. Heslop, M. K. Brenner, G. Dotti, CD28 costimulation improves expansion and persistence of chimeric antigen receptor–modified T cells in lymphoma patients. *J. Clin. Invest.* **121**, 1822–1826 (2011).
18. W. Liu, A. L. Putnam, Z. Xu-Yu, G. L. Szot, M. R. Lee, S. Zhu, P. A. Gottlieb, P. Kapranov, T. R. Gingeras, B. Fazekas de St Groth, C. Clayberger, D. M. Soper, S. F. Ziegler, J. A. Bluestone, CD127 expression inversely correlates with FoxP3 and suppressive function of human CD4⁺ T reg cells. *J. Exp. Med.* **203**, 1701–1711 (2006).
19. P. K. Chattopadhyay, M. R. Betts, D. A. Price, E. Gostick, H. Horton, M. Roederer, S. C. De Rosa, The cytolytic enzymes granzyme A, granzyme B, and perforin: Expression patterns, cell distribution, and their relationship to cell maturity and bright CD57 expression. *J. Leukoc. Biol.* **85**, 88–97 (2009).
20. T. Boettler, E. Panther, B. Bengsch, N. Nazarova, H. C. Spangenberg, H. E. Blum, R. Thimme, Expression of the interleukin-7 receptor α chain (CD127) on virus-specific CD8⁺ T cells identifies functionally and phenotypically defined memory T cells during acute resolving hepatitis B virus infection. *J. Virol.* **80**, 3532–3540 (2006).
21. R. J. Brentjens, E. Santos, Y. Nikhamin, R. Yeh, M. Matsushita, K. La Perle, A. Quintás-Cardama, S. M. Larson, M. Sadelain, Genetically targeted T cells eradicate systemic acute lymphoblastic leukemia xenografts. *Clin. Cancer Res.* **13**, 5426–5435 (2007).
22. M. Hallek, B. D. Cheson, D. Catovsky, F. Caligaris-Cappio, G. Dighiero, H. Döhner, P. Hillmen, M. J. Keating, E. Montserrat, K. R. Rai, T. J. Kipps; International Workshop on Chronic Lymphocytic Leukemia, Guidelines for the diagnosis and treatment of chronic lymphocytic

leukemia: A report from the International Workshop on Chronic Lymphocytic Leukemia updating the National Cancer Institute–Working Group 1996 guidelines. *Blood* **111**, 5446–5456 (2008).

23. H. Harada, M. M. Kawano, N. Huang, Y. Harada, K. Iwato, O. Tanabe, H. Tanaka, A. Sakai, H. Asaoku, A. Kuramoto, Phenotypic difference of normal plasma cells from mature myeloma cells. *Blood* **81**, 2658–2663 (1993).

24. R. Bataille, G. Jégo, N. Robillard, S. Barillé-Nion, J. L. Harousseau, P. Moreau, M. Amiot, C. Pellat-Deceunynck, The phenotype of normal, reactive and malignant plasma cells. Identification of "many and multiple myelomas" and of new targets for myeloma therapy. *Haematologica* **91**, 1234–1240 (2006).

25. J. R. Park, D. L. DiGiusto, M. Slovak, C. Wright, A. Naranjo, J. Wagner, H. B. Meechoovet, C. Bautista, W. C. Chang, J. R. Ostberg, M. C. Jensen, Adoptive transfer of chimeric antigen receptor re-directed cytolytic T lymphocyte clones in patients with neuroblastoma. *Mol. Ther.* **15**, 825–833 (2007).

26. M. A. Pule, B. Savoldo, G. D. Myers, C. Rossig, H. V. Russell, G. Dotti, M. H. Huls, E. Liu, A. P. Gee, Z. Mei, E. Yvon, H. L. Weiss, H. Liu, C. M. Rooney, H. E. Heslop, M. K. Brenner, Virus-specific T cells engineered to coexpress tumor-specific receptors: Persistence and antitumor activity in individuals with neuroblastoma. *Nat. Med.* **14**, 1264–1270 (2008).

27. B. L. Levine, L. M. Humeau, J. Boyer, R. R. MacGregor, T. Rebello, X. Lu, G. K. Binder, V. Slepushkin, F. Lemiale, J. R. Mascola, F. D. Bushman, B. Dropulic, C. H. June, Gene transfer in humans using a conditionally replicating lentiviral vector. *Proc. Natl. Acad. Sci. U.S.A.* **103**, 17372–17377 (2006).

28. A. P. Rapoport, E. A. Stadtmauer, N. Aqui, A. Badros, J. Cotte, L. Chrisley, E. Veloso, Z. Zheng, S. Westphal, R. Mair, N. Chi, B. Ratterree, M. F. Pochran, S. Natt, J. Hinkle, C. Sickles, A. Sohal, K. Ruehle, C. Lynch, L. Zhang, D. L. Porter, S. Luger, C. Guo, H. B. Fang, W. Blackwelder, K. Hankey, D. Mann, R. Edelman, C. Frasch, B. L. Levine, A. Cross, C. H. June, Restoration of immunity in lymphopenic individuals with cancer by vaccination and adoptive T-cell transfer. *Nat. Med.* **11**, 1230–1237 (2005).

29. A. Bondanza, V. Valtolina, Z. Magnani, M. Ponzoni, K. Fleischhauer, M. Bonyhadi, C. Traversari, F. Sanvito, S. Toma, M. Radrizzani, S. La Seta-Catamancio, F. Ciceri, C. Bordignon, C. Bonini, Suicide gene therapy of graft-versus-host disease induced by central memory human T lymphocytes. *Blood* **107**, 1828–1836 (2006).

30. L. Sabbagh, L. M. Snell, T. H. Watts, TNF family ligands define niches for T cell memory. *Trends Immunol.* **28**, 333–339 (2007).

31. L. Zitvogel, L. Apetoh, F. Ghiringhelli, G. Kroemer, Immunological aspects of cancer chemotherapy. *Nat. Rev. Immunol.* **8**, 59–73 (2008).

32. R. Ramakrishnan, D. Assudani, S. Nagaraj, T. Hunter, H. I. Cho, S. Antonia, S. Altiok, E. Celis, D. I. Gabrilovich, Chemotherapy enhances tumor cell susceptibility to CTL-mediated killing during cancer immunotherapy in mice. *J. Clin. Invest.* **120**, 1111–1124 (2010).

33. H. Wallen, J. A. Thompson, J. Z. Reilly, R. M. Rodmyre, J. Cao, C. Yee, Fludarabine modulates immune response and extends in vivo survival of adoptively transferred CD8 T cells in patients with metastatic melanoma. *PLoS ONE* **4**, e4749 (2009).

34. C. H. Lamers, R. Willemsen, P. van Elzakker, S. van Steenbergen-Langeveld, M. Broertjes, J. Oosterwijk-Wakka, E. Oosterwijk, S. Sleijfer, R. Debets, J. W. Gratama, Immune responses to transgene and retroviral vector in patients treated with ex vivo–engineered T cells. *Blood* **117**, 72–82 (2011).

35. J. L. Davis, M. R. Theoret, Z. Zheng, C. H. Lamers, S. A. Rosenberg, R. A. Morgan, Development of human anti-murine T-cell receptor antibodies in both responding and nonresponding patients enrolled in TCR gene therapy trials. *Clin. Cancer Res.* **16**, 5852–5861 (2010).

36. L. Naldini, U. Blömer, P. Gallay, D. Ory, R. Mulligan, F. H. Gage, I. M. Verma, D. Trono, In vivo gene delivery and stable transduction of nondividing cells by a lentiviral vector. *Science* **272**, 263–267 (1996).

37. P. L. Sinn, S. L. Sauter, P. B. McCray Jr., Gene therapy progress and prospects: Development of improved lentiviral and retroviral vectors—Design, biosafety, and production. *Gene Ther.* **12**, 1089–1098 (2005).

38. G. P. Wang, B. L. Levine, G. K. Binder, C. C. Berry, N. Malani, G. McGarrity, P. Tebas, C. H. June, F. D. Bushman, Analysis of lentiviral vector integration in HIV+ study subjects receiving autologous infusions of gene modified CD4+ T cells. *Mol. Ther.* **17**, 844–850 (2009).

39. S. Janetzki, C. M. Britten, M. Kalos, H. I. Levitsky, H. T. Maecker, C. J. Melief, L. J. Old, P. Romero, A. Hoos, M. M. Davis, "MIATA"—Minimal information about T cell assays. *Immunity* **31**, 527–528 (2009).

40. R. Zufferey, D. Nagy, R. J. Mandel, L. Naldini, D. Trono, Multiply attenuated lentiviral vector achieves efficient gene delivery in vivo. *Nat. Biotechnol.* **15**, 871–875 (1997).

41. G. G. Laport, B. L. Levine, E. A. Stadtmauer, S. J. Schuster, S. M. Luger, S. Grupp, N. Bunin, F. J. Strobl, J. Cotte, Z. Zheng, B. Gregson, P. Rivers, R. H. Vonderheide, D. N. Liebowitz, D. L. Porter, C. H. June, Adoptive transfer of costimulated T cells induces lymphocytosis in patients with relapsed/refractory non-Hodgkin lymphoma following CD34⁺-selected hematopoietic cell transplantation. *Blood* **102**, 2004–2013 (2003).